

# Dalton Transactions

Accepted Manuscript



This is an *Accepted Manuscript*, which has been through the Royal Society of Chemistry peer review process and has been accepted for publication.

*Accepted Manuscripts* are published online shortly after acceptance, before technical editing, formatting and proof reading. Using this free service, authors can make their results available to the community, in citable form, before we publish the edited article. We will replace this *Accepted Manuscript* with the edited and formatted *Advance Article* as soon as it is available.

You can find more information about *Accepted Manuscripts* in the [Information for Authors](#).

Please note that technical editing may introduce minor changes to the text and/or graphics, which may alter content. The journal's standard [Terms & Conditions](#) and the [Ethical guidelines](#) still apply. In no event shall the Royal Society of Chemistry be held responsible for any errors or omissions in this *Accepted Manuscript* or any consequences arising from the use of any information it contains.



[www.rsc.org/dalton](http://www.rsc.org/dalton)

## ARTICLE

# Synthesis, crystal structure and EPR spectroscopic analysis of novel copper complexes formed from *N*-pyridyl-4-nitro-1,8-naphthalimide ligands

Cite this: DOI: 10.1039/x0xx00000x

Received 00th January 2012,  
Accepted 00th January 2012

DOI: 10.1039/x0xx00000x

www.rsc.org/

Jonathan A. Kitchen<sup>a,b,\*</sup>, Paulo N. Martinho,<sup>c,d</sup> Grace G. Morgan,<sup>c</sup> and Thorfinnur Gunnlaugsson<sup>\*a</sup>

The mono-dentate, pyridyl containing, nitro naphthalimide ligands *N*-(4-pyridyl)-4-nitro-1,8-naphthalimide (**L**<sub>1</sub>) and *N*-(3-pyridyl)-4-nitro-1,8-naphthalimide (**L**<sub>2</sub>) were prepared and complexed with a selection of copper salts [Cu(OAc)<sub>2</sub>, Cu(CF<sub>3</sub>SO<sub>3</sub>)<sub>2</sub> and Cu(ClO<sub>4</sub>)<sub>2</sub>]. Crystallographic studies were undertaken and revealed that dinuclear acetate bridged complexes resulted from reactions with Cu(OAc)<sub>2</sub>, while mononuclear systems resulted from reactions with Cu(CF<sub>3</sub>SO<sub>3</sub>)<sub>2</sub> and Cu(ClO<sub>4</sub>)<sub>2</sub>. Despite the differing coordination environments the naphthalimide based ligands provided a range of interesting  $\pi$ -based interactions in the form of  $\pi\cdots\pi$ , anion $\cdots\pi$ , nitro $\cdots\pi$ , solvent $\cdots\pi$  and C=O $\cdots\pi$  associations. Solid state EPR spectra were in agreement with the coordination environments observed from crystallography.

## Introduction

The properties of *N*-substituted-1,8-naphthalimide derivatives have elegantly been put to use in many areas of chemistry including, but not limited to, fluorescent sensors for anions and cations, logic gate mimics, optical brighteners, electroluminescent species, intracellular imaging agents, DNA binders and probes.<sup>1-4</sup> More recently naphthalimide derivatives have been utilised as building blocks in metal based supramolecular architectures where their  $\pi$ -deficient nature and ability to be readily functionalised has been exploited giving rise to systems in which the extension of the structure occurs through  $\pi$ -based interactions. This work has largely been pioneered by Reger and co-workers who, over the last decade, have functionalized the 1,8-naphthalimide moiety at the imide nitrogen site, with various transition metal ion coordinating functional groups such as carboxylates,<sup>5-14</sup> pyrazoles<sup>15-19</sup> and other coordinating groups,<sup>20</sup> and studied the structural aspects of the resulting complexes.

Of particular note, is the series of paddle wheel complexes prepared using carboxylate containing  $\pi$ -deficient 1,8-naphthalimide ligands (as the equatorial components of the paddle wheel). These systems, which contain dinuclear paddlewheel units of Cu(II), Zn(II), Rh(III), have been structurally investigated where it was found that the naphthalimide portions act as secondary building units (SBU's) to extend the structure through non-covalent interactions ( $\pi$ -based interactions). Whilst Reger and co-workers have studied their naphthalimide-based systems using non-aromatic substituted ligands, we have focused our recent effort in this area on the development of 4-substituted naphthalimide ligands. This is particularly attractive, as such compounds (e.g. 4-nitro

and 4-amino-1,8-naphthalimides) possess highly desirable photophysical properties and the 4-position can be readily manipulated to introduce additional functionality, such as pyridyl coordination sites. To this end we have actively been involved in the use of naphthalimide based ligands to prepare novel transition metal complexes, for sensing, as probes for DNA binding, as cellular imaging agents, as well as developing them further to give naphthalimide containing Tröger's base derivatives.<sup>21-35</sup> With the view of exploring the possibility of incorporating such ligands into larger coordinating networks, metallo organic frameworks or supramolecular complexes, we embarked on the development of novel structurally simple naphthalimide ligands. Herein we report the synthesis of monodentate pyridyl containing 4-substituted naphthalimide based ligands **L**<sub>1</sub> and **L**<sub>2</sub> and the resulting complexation studies with Cu(II) metal salts [Cu(OAc)<sub>2</sub>, Cu(ClO<sub>4</sub>)<sub>2</sub>·6H<sub>2</sub>O and Cu(CF<sub>3</sub>SO<sub>3</sub>)<sub>2</sub>] in order to assess their applicability as synthons in developing higher order supramolecular architectures. The two ligands were designed for the following reasons; *a*) the use of the nitro naphthalimide would give rise to the possibility of introducing alternative supramolecular binding interactions as well as *b*) the two pyridine isomers would add directionality to the overall self-assembly interactions. Indeed, we demonstrate, using X-ray crystallography, that unlike previous examples in the literature, these nitro containing naphthalimide ligands have additional  $\pi$ -based interactions involving the imide rings and neighbouring nitro groups, opening up a new avenue for applications of naphthalimides in coordination chemistry.

## Results and discussion

### Ligand synthesis

**Scheme 1.** Synthetic procedure for the synthesis of ligands **L**<sub>1</sub> and **L**<sub>2</sub>. (a) 4-Aminopyridine, toluene, Et<sub>3</sub>N, molecular sieves, reflux; (b) 3-Aminopyridine, toluene, Et<sub>3</sub>N, molecular sieves, reflux; (c) CH<sub>3</sub>CN, excess benzyl bromide, 60°C.

The ligands, 4-nitro-1,8-naphthalimide-pyrid-4-yl (**L**<sub>1</sub>) and 4-nitro-1,8-naphthalimide-pyrid-3-yl (**L**<sub>2</sub>) were synthesised as shown in Scheme 1. In accordance to our reported general procedure,<sup>35</sup> the reaction of 4-nitro-1,8-naphthalic anhydride with either 4-amino-pyridine or 3-amino pyridine in refluxing toluene (anhydrous) for 3 days gave **L**<sub>1</sub> and **L**<sub>2</sub> as analytically pure yellow/orange microcrystalline solids in 40% and 50% yields respectively after standard acid-base workup and recrystallisation from methanol. Both **L**<sub>1</sub> and **L**<sub>2</sub> were fully characterised by using 1D and 2D NMR experiments, as well as IR spectroscopy, microanalysis and mass spectrometry. The absorption and the emission spectra were also recorded (see ESI for **L**<sub>1</sub>); these were typical of that seen for 4-nitro-1,8-naphthalimide based structures,<sup>1</sup> a broad absorption band with  $\lambda_{\max}$  at 350 nm and a small shoulder in the 450 nm region when

recorded in CH<sub>3</sub>CN. Upon excitation of the  $\lambda_{\max}$  a broad fluorescence emission was observed between 360 and 600 nm, with  $\lambda_{\max}$  at 450 nm. The pyridyl absorption occurred at higher energy and being masked by the high-energy naphthalimide transitions. Being orthogonal (see below) to the naphthalimide rings the pyridyl unit does not contribute to overall emission properties of the ligand (see ESI for **L**<sub>1</sub>).

In order to obtain crystallographic evidence for the formation of **L**<sub>1</sub> and **L**<sub>2</sub>, both ligands were quarternerized at the pyridyl nitrogen atoms by heating in CH<sub>3</sub>CN with benzyl bromide (60°C). Good quality orange block like crystals of **L**<sub>1</sub>**Bn**·**Br** were obtained by slow evaporation of the reaction solution and poor quality yellow blocks of **L**<sub>2</sub>**Bn**·**Br** by diffusion of diethylether into the reaction solution. The quarternerized compound **L**<sub>1</sub>**Bn**·**Br** crystallized in the monoclinic space group C2/c and contained one molecule in the asymmetric unit, Figure 1. As expected the ligand is not completely planar as the mean planes formed between the 4-pyridyl-ring and the naphthalimide core intersect at 55.23°.

The oxygen atoms of the 4-nitro group are disordered over two sites with relative occupancies of 0.65 and 0.35. Many packing interactions exist in **L**<sub>1</sub>**Bn**·**Br**, including  $\pi$ ··· $\pi$  stacking, anion··· $\pi$  interactions, NO<sub>2</sub>··· $\pi$  interactions and non-classical CH hydrogen bonding. Of particular note are the  $\pi$ ··· $\pi$  interactions formed by the naphthalene portion of **L**<sub>1</sub> and the interactions (NO<sub>2</sub>··· $\pi$  and Br··· $\pi$ ) to the diimide portion. Molecules of **L**<sub>1</sub>**Bn**·**Br** pack into dimers through weak  $\pi$ ··· $\pi$  stacking between the naphthalene rings [centroid···centroid = 3.697 Å] and NO<sub>2</sub>··· $\pi$  interactions [O(1)···centroid = 3.282 Å and O(20)···centroid = 3.114 Å], (see ESI). In addition, the opposite face of the naphthalimide is involved in a weaker  $\pi$ ··· $\pi$  interaction [centroid···centroid = 3.727 Å] and a Br··· $\pi$  interaction [Br···centroid = 3.412 Å]. The aforementioned  $\pi$ ··· $\pi$  interaction also places two nitro groups from the adjacent molecules in close proximity giving a N···O distance of 2.959 Å.<sup>36</sup> **L**<sub>2</sub>**Bn**·**Br** crystallized in the monoclinic space P21/n and contained one molecule in the asymmetric unit and one interstitial acetonitrile molecule. Packing interactions are slightly different in **L**<sub>2</sub>**Bn**·**Br** compared to **L**<sub>1</sub>**Bn**·**Br** as only  $\pi$ ··· $\pi$  stacking (weak  $\pi$ ··· $\pi$  interaction between the diimide ring and an adjacent naphthalene ring and non-classical CH hydrogen bonding interactions are observed (see Supporting Information). The structures of these two ligand systems are rich in interesting short contacts;  $\pi$ ··· $\pi$  stacking, CH hydrogen bonding, NO<sub>2</sub>··· $\pi$  interactions, NO<sub>2</sub>···NO<sub>2</sub> interactions, and anion··· $\pi$  interactions. This suggests that they are ideally suited for the preparation of new metal-based supramolecular architectures as multiple interesting intermolecular interactions are possible. Following full characterization of the two ligands

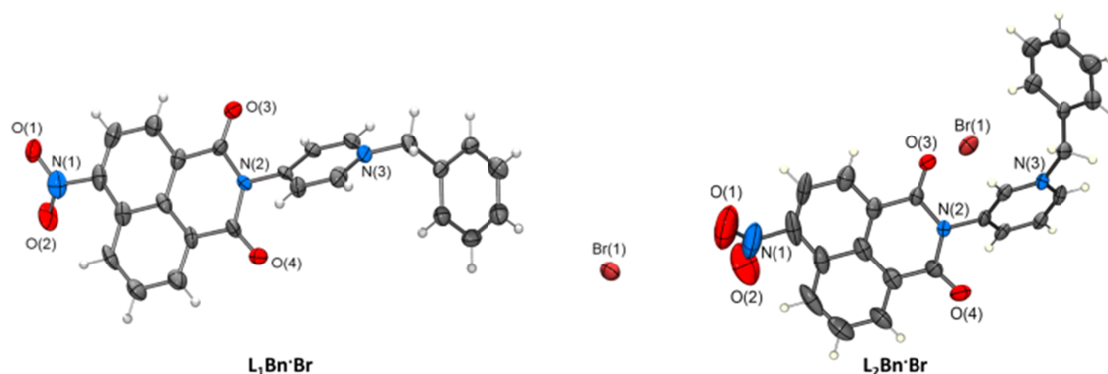
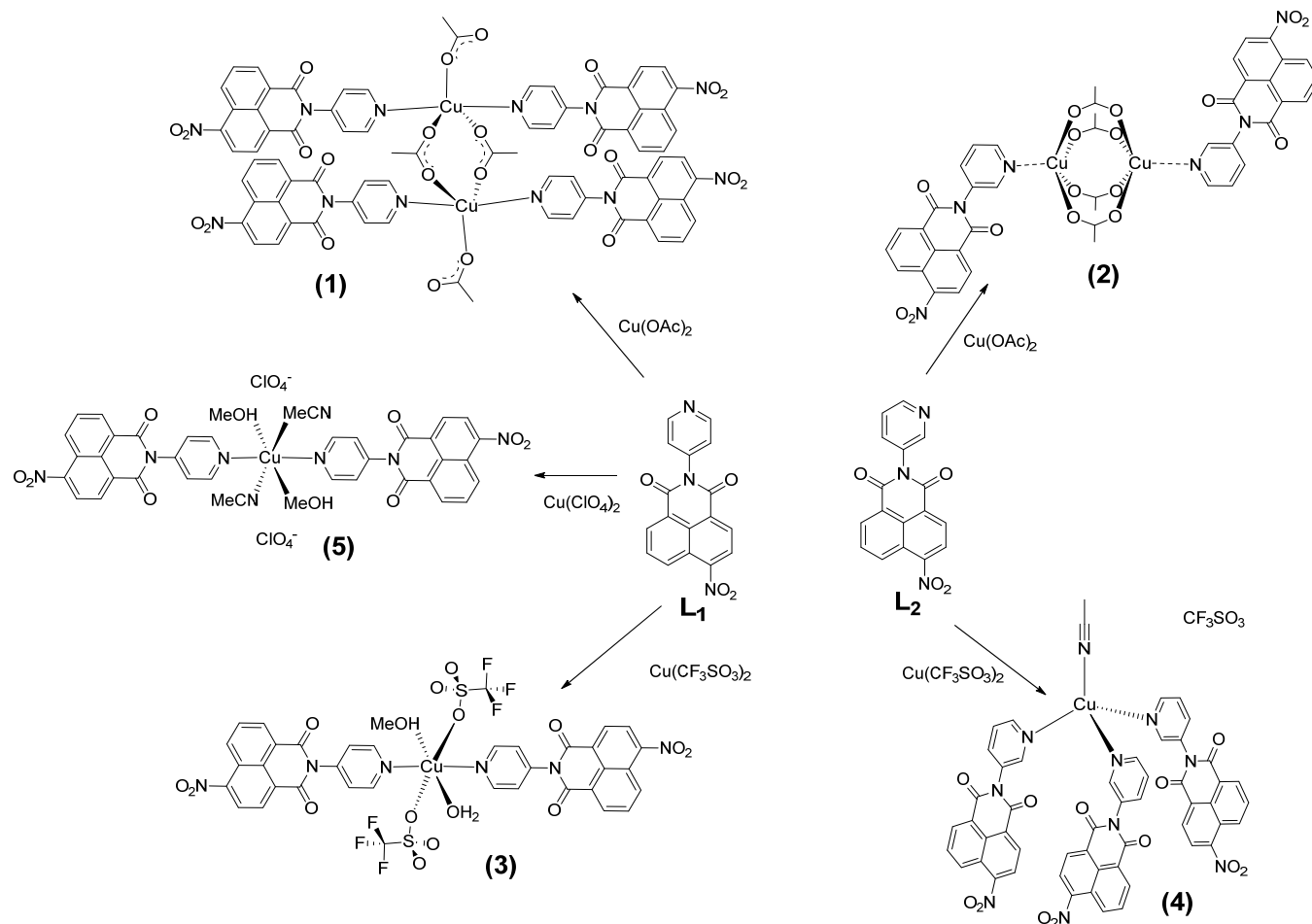


**Figure 1.** Perspective views of **L**<sub>1</sub>**Bn**·**Br** (left) and **L**<sub>2</sub>**Bn**·**Br** (right) with probability ellipsoids shown at 50%



**Scheme 2.** Overview of complexation reactions carried out between ligands  $L_1$  and  $L_2$  and a variety of Cu(II) salts. All reactions carried out in  $\text{CH}_3\text{CN}:\text{MeOH}$  (1:1) solution.

their Cu(II) complexes with a variety of Cu(II) salts were prepared and characterised.

### Cu(II) complexation studies of ligands $L_1$ and $L_2$

The two ligands  $L_1$  and  $L_2$  which differed only in the nature of the pyridyl binding group (3- or 4-pyridyl) were reacted with copper(II) salts  $\text{Cu}(\text{OAc})_2$ ,  $\text{Cu}(\text{ClO}_4)_2 \cdot 6\text{H}_2\text{O}$  and  $\text{Cu}(\text{CF}_3\text{SO}_3)_2$  in order to assess the binding nature of these monodentate ligands and, in particular, analyse how the large  $\pi$ -deficient nitro-naphthalimide based ligands, in conjunction with different counteranions can influence the stoichiometry, nuclearity and the packing of the resulting complexes, as depicted in Scheme 2.

Ligands  $L_1$  and  $L_2$  were reacted in 2:1 stoichiometric ratios with the various Cu(II) salts in a refluxing solvent mixture of (anhydrous)  $\text{CH}_3\text{CN}/\text{MeOH}$  (1:1) for 1 hour. After cooling to room temperature the orange or green mixtures were filtered through celite to remove a fine brown solid and subjected to vapour diffusion with diethyl ether. In most cases the complexes formed bulk samples of single crystals (with a fine brown powder also present, which was of unknown composition, and not analysed any further) and were isolated as crystalline samples after careful physical separation from the fine brown powder therefore the stoichiometry was determined through single crystal X-ray diffraction studies. In each case the only variable was the Cu(II) metal salt used as other reaction

conditions (*i.e.* concentrations, reaction times, solvent systems and isolation methods) were constant.

Reaction of  $L_1$  and  $L_2$  with  $\text{Cu}(\text{OAc})_2$  gave dinuclear complexes for both ligands. However, the formulation, bridging and coordination geometries of the Cu(II) centres were quite different in each complex.  $L_1$  gave a neutral, tetra-ligand complex with two bridging and two terminal acetate molecules  $[\text{Cu}_2^{\text{II}}(\text{L}_1)_4(\mu\text{-OAc})_2(\text{OAc})_2]$  (**1**), in 40 % yield while  $L_2$  resulted in a ‘paddle wheel’ complex with two molecules of  $L_2$  as the axial components  $[\text{Cu}_2^{\text{II}}(\text{L}_2)_2(\mu\text{-OAc})_4]$  (**2**) in 37 % yield, thereby demonstrating that a subtle change to the ligand results in a marked difference in the complexes. In agreement with this, the reaction of  $L_1$  and  $L_2$  with  $\text{Cu}(\text{CF}_3\text{SO}_3)_2$  resulted in mononuclear complexes where the nature of the complexes were again very different.

Using ligand  $L_1$  resulted in the formation of a neutral, octahedral Cu(II) complex where two ligands, two methanol molecules and two triflate counter anions were bound to the Cu(II) centre, resulting in the formation of  $[\text{Cu}^{\text{II}}(\text{L}_1)_2(\text{MeOH})(\text{H}_2\text{O})(\text{CF}_3\text{SO}_3)_2]$  (**3**), in 29 % yield. When  $L_2$  was reacted under the same conditions, the result was a mononuclear, tetrahedral Cu(I) complex with three ligands and one  $\text{CH}_3\text{CN}$  bound,  $[\text{Cu}^{\text{I}}(\text{L}_2)_3(\text{CH}_3\text{CN})](\text{CF}_3\text{SO}_3)$  (**4**), in 58 % yield. This further demonstrates that the subtle ligand change dramatically alters the outcome of the product.‡

In an analogous manner, the complexation of  $L_1$  with  $\text{Cu}(\text{ClO}_4)_2 \cdot 6\text{H}_2\text{O}$  resulted in green/blue crystals of a



mononuclear octahedral Cu(II) complex,  $[\text{Cu}^{\text{II}}(\text{L}_1)_2(\text{MeOH})_2(\text{CH}_3\text{CN})_2](\text{ClO}_4)_2$  (**5**), in 48 % yield. In this case two ligand molecules and four solvent molecules made up the coordination sphere. Despite many attempts using a large range of different solvent combinations and crystallisation techniques, single crystals from the reaction of  $\text{L}_2$  with  $\text{Cu}(\text{ClO}_4)_2 \cdot x\text{H}_2\text{O}$  could not be obtained. In each case green to yellow/brown powders were obtained, therefore the exact nature of this complex is unknown.

### Crystallographic analysis of complexes

Large dark green block shaped crystals of **1** were obtained from diffusion of diethyl ether directly into the  $\text{CH}_3\text{CN}/\text{MeOH}$  (1:1) reaction solution and the X-ray crystal structure was determined at 108 K. The complex crystallises in the triclinic space group P-1 and contains half of one molecule in the asymmetric unit with the other half generated by a centre of inversion, as demonstrated in Figure 2.

The structure revealed a dinuclear configuration in which the two Cu(II) centres each have three bound acetates (two bridging and one terminal) and two bound molecules of  $\text{L}_1$  to give an  $\text{N}_2\text{O}_3$  coordination sphere. The bridging acetates adopt an asymmetric binding mode with one oxygen atom having a *syn* binding mode and the other intermediate between purely *syn* and purely *anti*-. This binding mode results in a Cu...Cu separation of 4.478(2) Å which is slightly longer than observed in paddle wheel arrangements (*syn-syn* binding) where the Cu...Cu distance is typically < 3 Å, and slightly shorter than observed for *syn-anti* binding (~4.99 Å).

The coordination geometry of the copper centres is best described as highly distorted square based pyramidal with the degree of trigonality ( $\tau$ ) calculated to be 0.37 ( $\tau = 1.0$  for regular trigonal bipyramidal and 0.0 for regular square based pyramidal).<sup>37</sup> The basal plane comprises the two bound pyridyl nitrogen atoms (N(3) and N(23)), the terminally bound acetate (O(40)) and the *syn*-bound oxygen atoms from the bridging

acetate (O(50)). The bond lengths of the basal plane fall within 1.931(2) – 2.023(2) Å and the *cis* angles are all close to 90° [range = 89.0(1) – 91.5(1)°]. The axial position is occupied by the “*anti*” bound oxygen atom (O(51)) of a bridging acetate, and with a bond length of 2.282(2) Å it is significantly longer than the equatorial bonds. The *cis* angles formed to the axial group deviate significantly from 90° [87.2(1) – 108.9(1)°]. The structure contains no interstitial solvent molecules; however one of the two crystallographically independent ligand molecules contains disorder.

Packing interactions in **1** are governed primarily by interactions to the  $\pi$ -deficient naphthalimide moiety. The imide ring is involved in both  $\text{C}=\text{O} \cdots \pi$ , anion  $\cdots \pi$  and  $\text{NO}_2 \cdots \pi$  interactions, the former being intra-molecular and the latter two inter-molecular. Figure 2 shows the interactions involving the imide ring, where the carbonyl group of one ligand interacts with the ring of another within the same molecule [ $\text{C}=\text{O}(23) \cdots$ centroid distance is 3.114 Å]. Neighbouring molecules are then linked through a strong anion  $\cdots \pi$  interaction between the non-coordinated oxygen atom of the terminally bound acetate and the imide ring of a neighbouring complex molecule [ $\text{O}(41) \cdots$ centroid = 2.703 Å]. In addition there is also a  $\text{NO}_2 \cdots \pi$  interaction occurring in tandem with a weak offset face-to-face  $\pi \cdots \pi$  interaction between a second neighbouring molecule [ $\text{NO}(2) \cdots$ centroid = 2.920 Å and  $\pi \cdots \pi$  centroid to centroid = 3.663]. The overall result of the aforementioned  $\pi$ -based interactions is a step-like stacking of naphthalimide rings.

Small poor quality green blocks of **2** were grown from vapour diffusion of diethyl ether into the  $\text{CH}_3\text{CN}/\text{MeOH}$  reaction solution. The complex crystallizes in the triclinic space group P-1 and contains half of one molecule in the asymmetric unit with the other half generated by a centre of inversion. The low temperature (108 K) X-ray structure revealed a paddle wheel complex where four bridging acetates occupy the equatorial positions and two ligand molecules of  $\text{L}_2$  coordinate at the axial sites as shown in Figure 3.

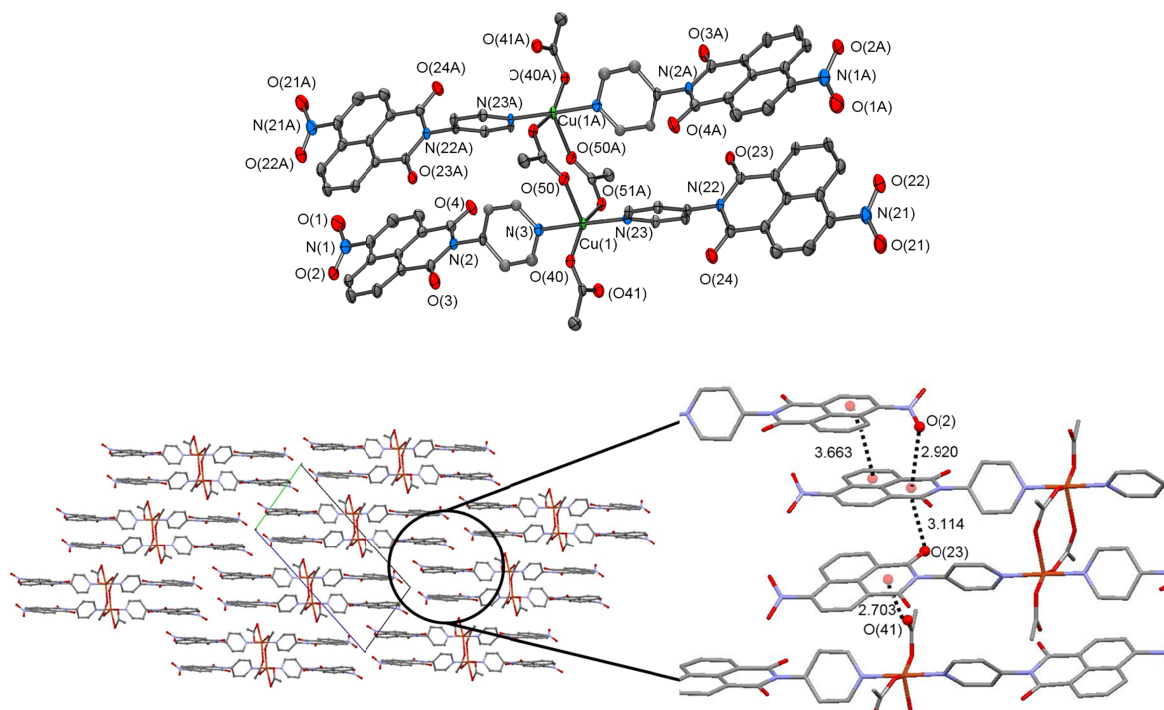


**Figure 2:** Perspective view (top) of the crystal structure of **1**, hydrogen atoms and disorder omitted for clarity. Packing interactions (bottom) in **1** highlighting anion  $\cdots \pi$ , nitro  $\cdots \pi$  and  $\pi \cdots \pi$  interactions involving the naphthalimide moiety described in main text.

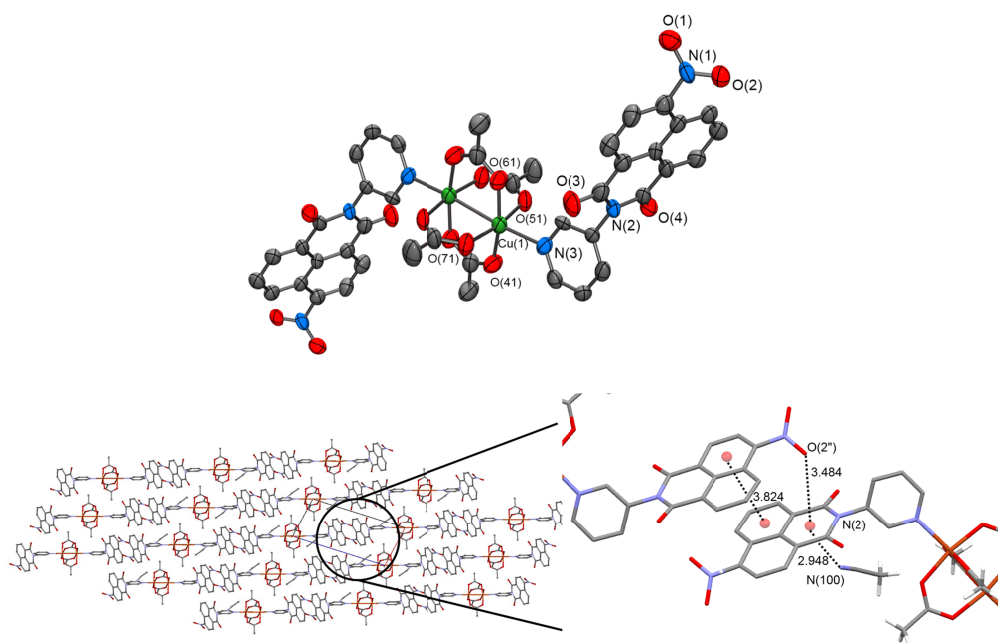


**Figure 3:** Perspective view (top) of the crystal structure of **2** (hydrogen atoms and interstitial solvent molecules omitted for clarity). Packing interactions (bottom) in **2** highlighting solvent $\cdots\pi$ , nitro $\cdots\pi$  and  $\pi\cdots\pi$  interactions involving the naphthalimide group.

The copper(II) centres in Figure 3, are best described as having square based pyramidal geometry with the acetate oxygen atoms in the equatorial square plane (av. Cu-O bond length = 1.985 Å), and the pyridyl nitrogen occupying the axial position [Cu(1)-N(3) = 2.241(8) Å]. The distance between the copper centres in this structure [2.632(2) Å] is much shorter than the previous structure (**1**). The mean plane formed between the 4-pyridyl ring and the naphthalimide is 70.8(2)°.

As was seen above, then there are many interesting packing interactions present within **2** primarily involving the  $\pi$ -system

of the naphthalimide core; a strong solvent $\cdots\pi$  interaction exists between the nitrogen atom of the interstitial acetonitrile and one face of the naphthalimide ring [N(100) $\cdots$ centroid = 2.948 Å]. The other face of the naphthalimide ring is involved in a weak  $\pi\cdots\pi$  interactions to a symmetry generated naphthalimide ring on a neighbouring complex [centroid $\cdots$ centroid = 3.824 Å]. In addition there is an interaction between the disordered nitro groups on one molecule and the imide portion of the naphthalimide on the neighbouring molecule [O(2) $\cdots$ centroid = 3.484 Å and O(11) $\cdots$ centroid = 3.031 Å]. These interactions

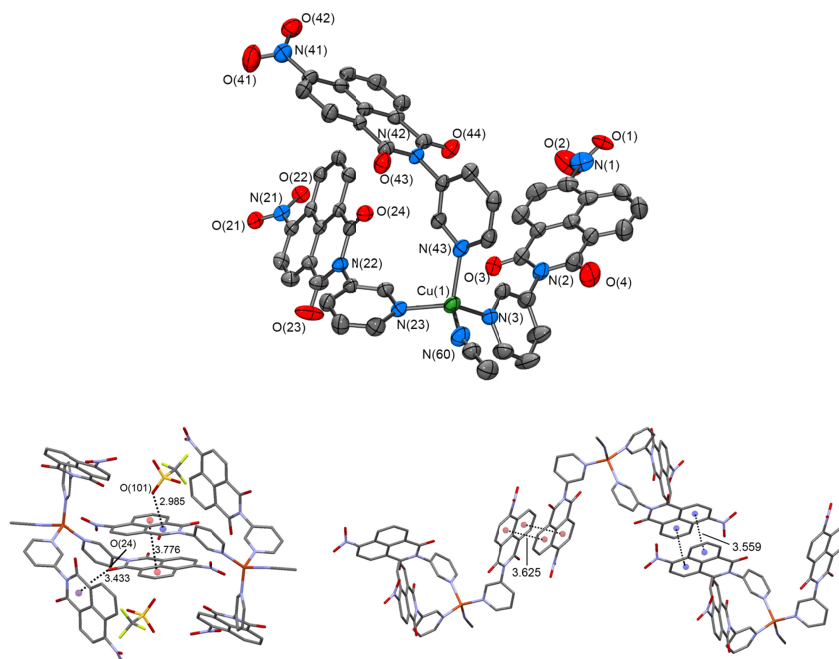


**Figure 4:** Perspective view (top) of the crystal structure of **4** (hydrogen atoms and  $\text{CF}_3\text{SO}_3^-$  anion omitted for clarity). Packing interactions (bottom) in **4** highlighting anion $\cdots\pi$ , C=O $\cdots\pi$  and  $\pi\cdots\pi$  interactions involving the naphthalimide rings.

align the molecules into chains in a step like arrangement. These stepped chains interact with neighbouring chains through nitro-carbonyl short contacts such that the carbonyl oxygen atom on one molecule is directed at the nitro group of a neighbouring molecule [ $O(4)\cdots N(1) = 2.987 \text{ \AA}$ ].

$N(1)$  and also between adjacent ligands of  $N(41)$ . In such interactions the naphthalene rings interact through weak offset face to face  $\pi\cdots\pi$  interactions [centroid $\cdots$ centroid =  $3.625 \text{ \AA}$  (for  $N(1)$ ) and  $3.559 \text{ \AA}$  (for  $N(41)$ )] and the head-to-tail nature of these interactions places the nitro groups above the diimide

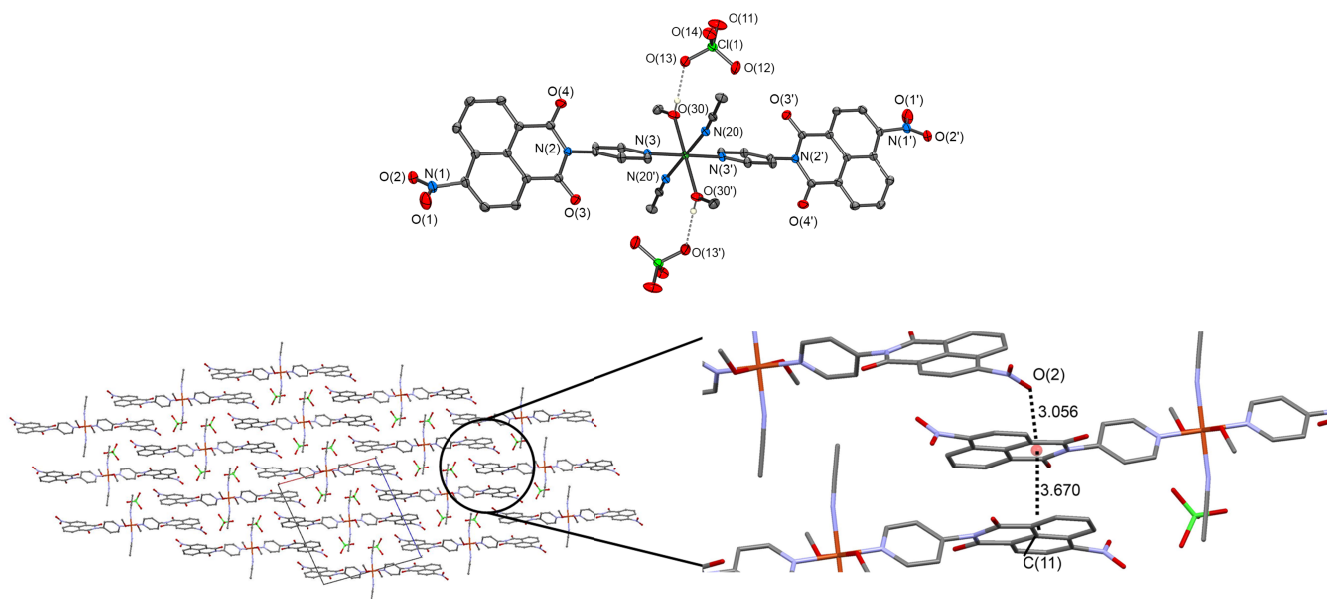


**Figure 5:** Perspective view (top) of **5** showing hydrogen bonding interactions between coordinated methanol and perchlorate counter anions (hydrogen atoms, other than MeOH, have been omitted for clarity). Packing interactions (bottom) in **5**, highlighting the nitro $\cdots\pi$  and  $\pi\cdots\pi$  interactions to the naphthalimide rings.

Small, very poor quality, green crystals of **3** were grown from the diffusion of diethyl ether into the  $\text{CH}_3\text{CN}/\text{MeOH}$  reaction solution. The complex crystallized in the triclinic space group P-1. The data was of such poor quality that very little structure description is presented. From the data the connectivity was established and showed that the  $\text{CF}_3\text{SO}_3^-$  counter anions are bound through oxygen atoms to the octahedral  $\text{Cu}(\text{II})$  centre (see ESI). Despite many attempts to isolate good quality single crystals no other solvent systems or crystallisation techniques gave crystals suitable for X-ray analysis.

Large orange/brown blocks of **4** were grown by the diffusion of diethyl ether into the  $\text{CH}_3\text{CN}/\text{MeOH}$  reaction solution. The complex crystallized in the triclinic space group P-1 with one molecule in the asymmetric unit. Three ligand molecules are arranged around the  $\text{Cu}(\text{I})$  with the remaining coordination site occupied by an acetonitrile molecule to give an overall  $\text{N}_4$  tetrahedral coordination environment. Bond lengths are within the typical range for  $\text{Cu}(\text{I})$  pyridyl complexes [ $2.008(4) - 2.075(4) \text{ \AA}$ ] and bond angles are within the expected range for a tetrahedral  $\text{Cu}(\text{I})$  complex [ $104.8(2) - 123.3(2)^\circ$ ]. There are no interstitial solvent molecules, however one of the three ligand molecules contains a disordered nitro group where the oxygen atoms are split over two positions (relative occupancies of 0.55 and 0.45). Just like the previous structures there are many interesting short contacts, many of which involve the naphthalimide rings. A short contact exists between the carbonyl oxygen of one ligand and the imide portion of another [ $O(24)\cdots\text{centroid} = 3.433 \text{ \AA}$ ] (Fig. 4). In this structure  $\pi\cdots\pi$  and nitro $\cdots\pi$  interactions exist in tandem between adjacent complex molecules such that there are two separate interactions of this type: between adjacent ligands of

portion of the ligands such that  $O(20)\cdots\text{centroid} = 3.111 \text{ \AA}$  (for ligand  $N(1)$ ) and  $O(42)\cdots\text{centroid} = 3.036 \text{ \AA}$  for ligand  $N(41)$ . The final type of interaction present is an anion $\cdots\pi$  interaction between the triflate counter anion and the imide portion of the ligand of  $N(23)$  [ $O(101)\cdots\text{centroid} = 2.985 \text{ \AA}$ ], Figure 4. The overall result of these inter-molecular packing interactions is a complex arrangement of these bulky molecules.

Pale green (plate like) crystals of **5** were obtained from the diffusion of diethyl ether into the  $\text{CH}_3\text{CN}/\text{MeOH}$  (1:1) reaction solution and the X-ray structure was determined at 108 K. The complex crystallises in the monoclinic space group P21/c and the asymmetric unit contains one half of the mononuclear complex with the other half generated through a centre of inversion. The mononuclear complex contains an octahedral  $\text{Cu}(\text{II})$  centre with two ligand molecules and two acetonitrile molecules occupying the equatorial plane and two axially bound methanol molecules giving an overall  $\text{N}_4\text{O}_2$  coordination sphere. The  $\text{Cu}(\text{II})$  is best described as a slightly elongated octahedral centre; the equatorial nitrogen based donors have an average bond length of  $2.027(2) \text{ \AA}$ , whilst the axial oxygen donors are significantly longer ( $2.262(2) \text{ \AA}$ ). The degree of tetragonality was calculated to be 0.89, a value consistent with slight elongation of the axial sites. The perchlorate counter anions are closely associated with the cationic complex through strong hydrogen bonding to the coordinated methanol molecules [ $O(30)\cdots O(13) = 2.757(2) \text{ \AA}$  and  $\angle(O(30)-H(30x)\cdots O(13) = 166^\circ$ ]. Again, crystal packing primarily involves short contacts to the  $\pi$ -deficient naphthalimide group in the form of  $\text{NO}_2\cdots\pi$  and  $\pi\cdots\pi$  interactions. The  $\pi\cdots\pi$  interactions between neighbouring naphthalimide rings are slightly different to those observed in the previous structures. Rather than the naphthalene portions of the ligand on top of

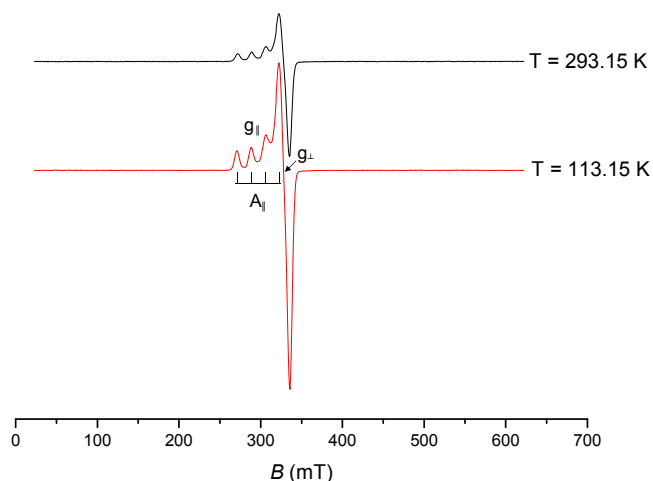


Figure 6. EPR spectra of solid sample of **5** at 113 K and 293 K.

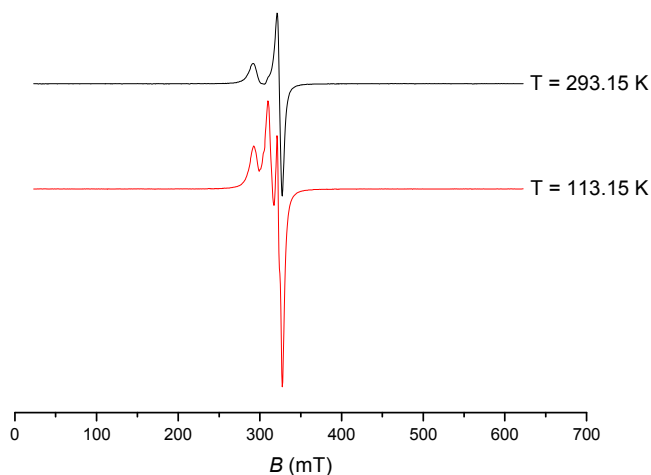


Figure 7. EPR spectra of solid sample of **1** at 113 K and 293 K.

each other, the ligands are slipped further such that the imide part on one overlaps with the naphthalene on the other [C(11)⋯centroid = 3.670 Å], Figure 5. The other face of the naphthalimide ring system involves a nitro⋯ $\pi$  interaction to the diimide part of the ring [O(2)⋯centroid = 3.056 Å], Figure 5.

Having structurally analysed all the complexes developed in this project, we next turned our attention to their EPR spectroscopy.

### EPR Spectroscopy

The X-band spectra of complexes **1-3** and **5** were all measured in the solid state at room temperature and at 113 K. The two mononuclear complexes **3** and **5** showed relatively simple spectra indicating axial geometry as would be expected from the regular geometry revealed in the crystal structure of **3**. Typical spectra are shown in Figure 6 for **5** (the result for **3** is given in the ESI); showing that at both high and low temperatures well resolved hyperfine coupling to the  $^{63}\text{Cu}$  and  $^{65}\text{Cu}$  nuclei on the  $g_{\parallel}$  component (17–19 G in all cases) was observed, which appears at lower field for all of the mononuclear complexes. As expected no hyperfine on the  $g_{\perp}$  component was observed.<sup>38</sup> In contrast, both the dinuclear complexes **1** and **2** show more complicated spectra; the spectra of complex **1** reflecting both the long internuclear distance

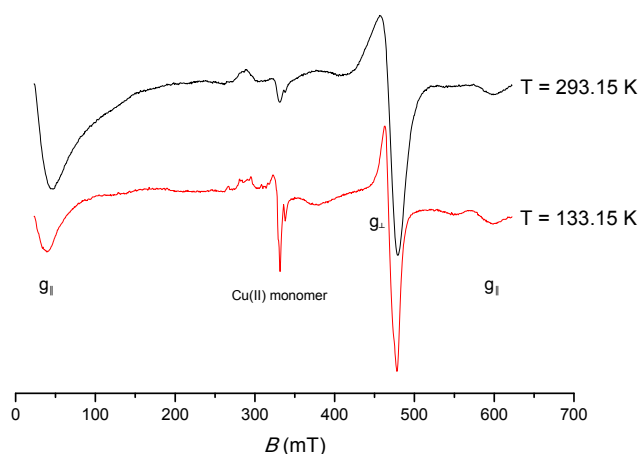


Figure 8. EPR spectra of solid sample of **1** at 113 K and 293 K.

(4.478(2) Å) between the pairs of five coordinate Cu(II) sites and the irregular geometry. The spectra at both temperatures, is shown in Figure 7, suggest two electronically independent copper sites in line with the crystallographic data which reveal a much longer internuclear distance than that in **2**. The short internuclear Cu–Cu distance of 2.632(2) Å and the quadruple acetate-bridging mode in **2** indicate that a strong interaction is likely between the two  $d^9$  centres and this is borne out by the X-band spectra at both temperatures, Figure 8. The dominant feature is a resonance at  $g_{\perp} = 1.44$  with additional signals at  $g = 17.9$  and  $g = 1.13$  representing the  $g_{\parallel}$  signal. The feature at  $g = 2.2$  is attributed to a mononuclear impurity,<sup>39</sup> but Skrzypek *et al.* have previously observed a very similar X-band spectrum for a related quadruply bridged dicopper(II) complex<sup>40</sup> and their analysis indicated strong antiferromagnetic coupling which is also likely for be the case for complex **2**.

### Conclusions

In this article we have presented several novel copper complexes from pyridyl 4-nitro-1,8-naphthalimide based ligands. These were formed by reacting ligands **L**<sub>1</sub> and **L**<sub>2</sub> and a selection of copper salts [Cu(OAc)<sub>2</sub>, Cu(CF<sub>3</sub>SO<sub>3</sub>)<sub>2</sub> and Cu(ClO<sub>4</sub>)<sub>2</sub>]; giving rise to a formation of a variety of complexes; all with differing coordination modes. Dinuclear acetate bridged complexes resulted from reactions with Cu(OAc)<sub>2</sub>, while mononuclear systems resulted from reactions with Cu(CF<sub>3</sub>SO<sub>3</sub>)<sub>2</sub> and Cu(ClO<sub>4</sub>)<sub>2</sub>. Despite the coordination environment, in each case the naphthalimide based ligands provided interesting  $\pi$ -based interactions in the form of  $\pi$ ⋯ $\pi$ , anion⋯ $\pi$ , nitro⋯ $\pi$ , solvent⋯ $\pi$  and C=O⋯ $\pi$  giving rise to extended structures through secondary interactions. Solid state EPR spectra of the four Cu(II) complexes were in agreement with the coordination environments observed from the X-ray crystallography of these structures. Of these, the mononuclear complexes **3** and **5** displayed typical spectra for mononuclear octahedral Cu(II) systems while dinuclear complexes **1** and **2** were more complex with **2** showing a spectrum indicative of strong antiferromagnetic coupling. In addition to the interesting  $\pi$ -based interactions that these systems yield, the ability to readily manipulate the substituents (both the coordination moiety at the diimide nitrogen atom and the 4-substituent of the naphthalene ring) also makes these ligands highly desirable for use in constructing complex supramolecular architectures. The results from our investigation clearly demonstrate that the



coordination groups can be manipulated in order to tune the properties of the bound metal (*e.g.* magnetic, photophysical and electrochemical properties, *etc.*) whilst the 4-position of the naphthalimide rings can be furnished with groups to impart additional functionality (*e.g.* ion receptors, reactive groups, functional groups to allow surface attachment); all opening up a major scope for developing novel metallo-supramolecular systems. The vast array of  $\pi$  based interactions shown in these complexes is encouraging as the extension of molecular networks through secondary binding interactions is an important area of supramolecular chemistry, in particular for the development of magnetically interesting compounds; an area that we are now actively pursuing.

## Experimental

### General Experimental

All chemicals were purchased from commercial sources and used as received. Solvents were HPLC grade and were used without further purification. Elemental analyses were carried out at the Microanalytical Laboratory, School of Chemistry and Chemical Biology, University College Dublin or at the Campbell Microanalytical Laboratory, University of Otago, New Zealand.

Infrared spectra were recorded on a Perkin-Elmer-Spectrum-One FT-IR spectrometer equipped with a Universal-ATR sampling accessory; solid samples were recorded directly as neat samples; in  $\text{cm}^{-1}$ .

NMR data were recorded on Bruker-DPX-400-Avance spectrometer (400.13 ( $^1\text{H}$ ) and 100.6 MHz ( $^{13}\text{C}$ )), in commercially available deuterated solvents;  $\delta$  in ppm relative to  $\text{SiMe}_4$  (= 0 ppm) referenced relative to the internal solvent signals,  $J$  in Hz; data were processed with Bruker Win-NMR 5.0 and Topspin 2.1 softwares.

X-ray data (Table 1) were collected on a Rigaku Saturn 724 CCD Diffractometer using graphite-monochromated Mo-K $\alpha$  radiation ( $\lambda = 0.71073 \text{ \AA}$ ). The data sets were collected using Crystalclear-SM 1.4.0 software. Data integration, reduction and correction for absorption and polarization effects were all performed using Crystalclear-SM 1.4.0 software. Space group determinations were obtained using Crystal structure ver. 3.8. The structures were solved by direct methods (SHELXS-97) and refined against all  $F^2$  data (SHELXL-97).<sup>41</sup> All H-atoms, except for O-H protons, were positioned geometrically and refined using a riding model with  $d(\text{CH}) = 0.95 \text{ \AA}$ ,  $U_{\text{iso}} = 1.2U_{\text{eq}}$  (C) for aromatic and  $0.98 \text{ \AA}$ ,  $U_{\text{iso}} = 1.2U_{\text{eq}}$  (C) for  $\text{CH}_3$ . Hydroxy protons were found from the difference map and fixed to the attached atoms with  $U_{\text{H}} = 1.2U_{\text{O}}$ . X-band electron paramagnetic resonance spectra of solid samples of compounds **1** – **3** and **5** were recorded at 293 and 113 K on a Magnetech Miniscope MS200 EPR spectrometer fitted with microwave frequency counter and a temperature controller. All measurements were performed with magnetic field centred at 322 mT and a field sweep of 600 mT.

**Caution:** While no problems were encountered in the course of this work, reactions involving  $\text{ClO}_4^-$  salts are potentially explosive so should be handled with appropriate care.

### Synthesis of **L**<sub>1</sub>, **L**<sub>2</sub> and their corresponding Cu(II) complexes:

#### *N*-(4-Pyridyl)-4-nitro-1,8-naphthalimide (**L**<sub>1</sub>)

4-Aminopyridine (0.263 g, 2.8 mmol) was added to a solution of 4-nitro-1,8-naphthalic anhydride (0.5 g, 2.0 mmol) and triethylamine (0.56 mL) in anhydrous toluene (50 mL). The

orange reaction mixture was stirred under argon at reflux for 3 days in the presence of 3  $\text{\AA}$  molecular sieves. The resulting dark red/brown reaction mixture was filtered through celite while hot and washed with 3  $\times$  50 mL aliquots of toluene. The toluene was removed under reduced pressure and the crude brown solid recrystallized from methanol to yield ligand **L**<sub>1</sub> as a pale orange microcrystalline solid (0.250 g, 39%). Anal. Calcd. For  $\text{C}_{17}\text{H}_9\text{N}_3\text{O}_4$  (319.06  $\text{g mol}^{-1}$ ): C 63.95, H 2.84, N 13.16. Found: C 64.18, H 2.57, N 12.86%. HRMS 320.0677 ( $[\text{M}+\text{H}]^+$ ,  $\text{C}_{17}\text{H}_{10}\text{N}_3\text{O}_4$  requires 320.0671); NMR  $\delta_{\text{H}}$  (600 MHz, DMSO- $d_6$ ), 8.79 (3H, m, 2 $\times$ pyH & 1 $\times$  napH), 8.68-8.60 (3H, m, 3 $\times$ napH), 8.16 (1H, t,  $J = 7.6 \text{ Hz}$ , napH), 7.53 (2H, d,  $J = 6.0 \text{ Hz}$ , 2 $\times$ pyH); NMR  $\delta_{\text{C}}$  (150 MHz, DMSO- $d_6$ ), 162.8, 161.9, 150.7, 149.4, 143.5, 131.8, 130.2, 129.7, 129.1, 128.7, 126.9, 124.4, 124.3, 123.1, 122.9; IR  $\nu_{\text{max}}$ (neat sample)/ $\text{cm}^{-1}$  1716, 1677, 1583, 1524, 1411, 1371, 1352, 1237, 1198, 1135, 1107, 1065, 993, 959, 917, 858, 812, 784, 756, 743, 713.

#### *N*-(3-Pyridyl)-4-nitro-1,8-naphthalimide (**L**<sub>2</sub>)

3-Aminopyridine (0.263 g, 2.8 mmol) was added to a solution of 4-nitro-1,8-naphthalic anhydride (0.5 g, 2.0 mmol) and triethylamine (0.56 mL) in anhydrous toluene (50 mL). The orange reaction mixture was stirred under argon at reflux for 3 days in the presence of 3  $\text{\AA}$  molecular sieves. The resulting dark red/brown reaction mixture was filtered through celite while hot and washed with 3  $\times$  50 mL aliquots of toluene. The toluene was removed under reduced pressure and the crude brown solid recrystallized from methanol to yield ligand **L**<sub>2</sub> as a yellow solid (0.400 g, 63%). Anal. Calcd. For  $\text{C}_{17}\text{H}_9\text{N}_3\text{O}_4$  (319.06  $\text{g mol}^{-1}$ ): C 63.95, H 2.84, N 13.16. Found: C 64.00, H 2.88, N 13.21%. HRMS 320.0676 ( $[\text{M}+\text{H}]^+$ ,  $\text{C}_{17}\text{H}_{10}\text{N}_3\text{O}_4$  requires 320.0671); NMR  $\delta_{\text{H}}$  (600 MHz, DMSO- $d_6$ ), 8.75 (1H, d,  $J = 6 \text{ Hz}$  1 $\times$  napH), 8.67-8.62 (4H, m, 2 $\times$ pyH and 2 $\times$ napH), 8.57 (1H, d,  $J = 6 \text{ Hz}$ , napH) 8.12 (1H, t,  $J = 6 \text{ Hz}$ , napH), 7.89 (1H, dd,  $J = 12$  and  $6 \text{ Hz}$ , pyH), 7.60 (1H, dd,  $J = 12$  and  $6 \text{ Hz}$ , pyH); NMR  $\delta_{\text{C}}$  (150 MHz, DMSO- $d_6$ ), 163.5, 162.6, 151.4, 150.2, 144.3, 132.5, 130.9, 130.5, 129.9, 129.5, 127.8, 125.2, 125.0, 123.6, 123.4; IR  $\nu_{\text{max}}$ (neat sample)/ $\text{cm}^{-1}$  1710, 1594, 1516, 1472, 1443, 1403, 1318, 1239, 1195, 1175, 1115, 1064, 1012, 903, 831, 785.

#### *N*-(4-pyridinium)-4-nitro-1,8-naphthalimide bromide (**L**<sub>1</sub>Bn·Br)

*N*-(4-pyridyl)-4-nitro-1,8-naphthalimide (**L**<sub>1</sub>) (0.020 mg, 0.06 mmol) was heated at 60°C with stirring in  $\text{CH}_3\text{CN}$  (10 mL). To the resulting orange solution was added excess benzyl bromide and heating with stirring continued for 2 hours. The now pale orange solution was cooled to room temperature and filtered through celite to remove a very small amount of a fine brown precipitate and left to evaporate at room temperature. Overnight a number of small yellow/orange crystals had formed (15 mg, 49%). HRMS 410.1139 ( $[\text{M}-\text{Br}]^+$ ,  $\text{C}_{24}\text{H}_{16}\text{N}_3\text{O}_4$  requires 410.1141); NMR  $\delta_{\text{H}}$  (400 MHz, DMSO- $d_6$ ), 9.47 (2H, d,  $J = 7 \text{ Hz}$ , 2 $\times$ pyH), 8.84 (1H, dd,  $J = 1, 8 \text{ Hz}$  1 $\times$ napH), 8.73-8.63 (3H, m, 3 $\times$ napH), 8.37 (2H, d,  $J = 7 \text{ Hz}$ , 2 $\times$ pyH), 8.19 (1H, t,  $J = 8, 1 \times$ napH), 7.67 (2H, dd,  $J = 2, 8 \text{ Hz}$ , 2 $\times$ PhH), 7.53 (3H, m, 3 $\times$ PhH); NMR  $\delta_{\text{C}}$  (100 MHz, DMSO- $d_6$ ), 162.9, 162.1, 151.5, 150.2, 146.9, 134.4, 132.7, 130.8, 130.6, 130.2, 130.1, 129.9, 129.7, 129.2, 126.9, 124.8, 123.4, 123.0, 64.0. IR  $\nu_{\text{max}}$ (neat sample)/ $\text{cm}^{-1}$  2991, 2932, 1721, 1683, 1629, 1583, 1533, 1509, 1493, 1461, 1452, 1428, 1408, 1350, 1235, 1185, 1146, 1031, 942, 894, 845, 792, 776, 753



***N*-(3-pyridinium)-4-nitro-1,8-naphthalimide bromide (L<sub>2</sub>Bn·Br)**

*N*-(3-pyridyl)-4-nitro-1,8-naphthalimide (L<sub>2</sub>) (0.050 mg, 0.16 mmol) was heated at 60°C with stirring in CH<sub>3</sub>CN (20 mL). To the resulting pale yellow solution was added excess benzyl bromide and heating with stirring continued for 2 hours. The now bright yellow solution was cooled to room temperature and left to evaporate at room temperature resulting in a yellow powder (76 mg, quantitative yield). HRMS 410.1143 ([M-Br]<sup>+</sup>, C<sub>24</sub>H<sub>16</sub>N<sub>3</sub>O<sub>4</sub> requires 410.1141); NMR δ<sub>H</sub> (600 MHz, DMSO-d<sub>6</sub>), 9.46 (2H, m, 2 × pyH), 8.85 (2H, d, Hz 2 × pyH), 8.73 (2H, m, napH), 8.65 (1H, d, J = 6 Hz, napH), 8.48 (1H, dd, J = 12 and 6 Hz, pyH), 8.20 (1H, dd, J = 12 and 6 Hz, napH), 7.58 (2H, t, J = 6 Hz, 2 × PhH), 7.49 (3H, m, 3 × PhH), 6.03 (2H, s, CH<sub>2</sub>); NMR δ<sub>C</sub> (150 MHz, DMSO-d<sub>6</sub>), 163.2, 162.4, 150.1, 147.4, 145.7, 135.8, 134.2, 132.6, 130.6, 130.5, 130.1, 129.9, 129.7, 129.3, 129.0, 126.7, 124.7m 123.3, 122.9, 64.3; IR ν<sub>max</sub>(neat sample)/cm<sup>-1</sup> 2989, 2936, 1718, 1679, 1631, 1584, 1530, 1509, 1493, 1467, 1455, 1424, 1409, 1349, 1235, 1183, 1144, 1029, 943, 894, 845, 797, 781, 755, 742, 719, 706, 683.

**[Cu<sub>2</sub>(L<sub>1</sub>)<sub>4</sub>(μ-OAc)<sub>2</sub>(OAc)<sub>2</sub>] (1)**

Ligand L<sub>1</sub> (32 mg, 0.1 mmol) was dissolved in 20 mL CH<sub>3</sub>CN/MeOH (1:1) and heated to reflux with stirring. Solid copper(II) acetate (9 mg, 0.05 mmol) was added to the pale orange ligand solution and heating continued for a further 2 hours, after which the solution was subjected to vapour diffusion of diethyl ether. Large dark green crystals (17 mg, 40 %) were obtained after careful separation from a brown solid. Anal. Calcd. For [Cu<sub>2</sub>(C<sub>17</sub>H<sub>9</sub>N<sub>3</sub>O<sub>4</sub>)<sub>4</sub>(CH<sub>3</sub>CO<sub>2</sub>)<sub>4</sub>·2H<sub>2</sub>O (1674.17 gmol<sup>-1</sup>): C 54.47, H 3.13, N 10.03. Found: C 54.78, H 2.82, N 9.66%. IR ν<sub>max</sub>(neat sample)/cm<sup>-1</sup> 1701, 1683, 1599, 1517, 1433, 1375, 1350, 1244, 1201, 1021, 916, 866, 783, 759, 720, 705, 678.

**[Cu<sub>2</sub>(L<sub>2</sub>)<sub>2</sub>(μ-OAc)<sub>4</sub>·2MeCN (2)**

Ligand L<sub>2</sub> (32 mg, 0.1 mmol) was dissolved in 20 mL CH<sub>3</sub>CN/MeOH (1:1) and heated to reflux with stirring. Solid copper(II) acetate (9 mg, 0.05 mmol) was added to the yellow ligand solution and heating continued for a further 2 hours. The solution was subjected to vapour diffusion of diethyl ether, resulting in large green/blue block shaped crystals (20 mg, 37%). Anal. Calcd. For [Cu<sub>2</sub>(C<sub>17</sub>H<sub>9</sub>N<sub>3</sub>O<sub>4</sub>)<sub>2</sub>(CH<sub>3</sub>CO<sub>2</sub>)<sub>4</sub>·2CH<sub>3</sub>CN (1082.08 gmol<sup>-1</sup>): C 51.01, H 3.35, N 10.35. Found: C 51.61, H 3.35, N 9.75%. IR ν<sub>max</sub>(neat sample)/cm<sup>-1</sup> 1709, 1671, 1617, 1588, 1523, 1426, 1371, 1348, 1238, 1196, 1028, 908, 853, 784, 758, 721, 702, 677.

**[Cu(L<sub>1</sub>)<sub>2</sub>(MeOH)(H<sub>2</sub>O)(CF<sub>3</sub>SO<sub>3</sub>)<sub>2</sub>] (3)**

Ligand L<sub>1</sub> (32 mg, 0.10 mmol) was dissolved in 20 mL CH<sub>3</sub>CN/MeOH (1:1) and stirred at reflux while a methanolic solution (1 mL) of Cu(CF<sub>3</sub>SO<sub>3</sub>)<sub>2</sub> (18 mg, 0.05 mmol) was added. No major colour change was observed and the resulting orange solution was stirred at reflux for 1 hour before being filtered and subjected to vapour diffusion of diethyl ether. After one week a bright green crystalline solid was obtained in low yield after careful separation from a yellow powder (15 mg, 29%).

Anal.	Calcd.	For
[Cu(C <sub>17</sub> H <sub>9</sub> N <sub>3</sub> O <sub>4</sub> ) <sub>2</sub> (CH <sub>3</sub> OH)(H <sub>2</sub> O)(CF <sub>3</sub> SO <sub>3</sub> ) <sub>2</sub> ] (1048.98 gmol <sup>-1</sup> ):		
C 42.33, H 2.31, N 8.01.	Found: C 42.53, H 2.28, N 8.27%.	
IR ν <sub>max</sub> (neat sample)/cm <sup>-1</sup> 3445, 3081, 1717, 1663, 1621, 1595, 1525, 1488, 1421, 1411, 1366, 1348, 1238, 1195, 1033, 910, 870, 855, 831, 806, 781, 759, 720, 705, 677.		

**[Cu(L<sub>2</sub>)<sub>3</sub>CH<sub>3</sub>CN]CF<sub>3</sub>SO<sub>3</sub> (4)**

Ligand L<sub>2</sub> (32 mg, 0.10 mmol) was dissolved in 20 mL CH<sub>3</sub>CN/MeOH (1:1) and stirred at reflux while a methanolic solution (1 mL) of Cu(CF<sub>3</sub>SO<sub>3</sub>)<sub>2</sub> (18 mg, 0.05 mmol) was added. No major colour change was observed and the resulting clear orange solution was stirred at reflux for 1 hour before being subjected to vapour diffusion of diethyl ether. A large number of brown crystals were obtained without the need to separate from a yellow powder (30 mg, 58 %). Anal. Calcd. For [Cu(C<sub>17</sub>H<sub>9</sub>N<sub>3</sub>O<sub>4</sub>)<sub>3</sub>(CH<sub>3</sub>CN)](CF<sub>3</sub>SO<sub>3</sub>)·2H<sub>2</sub>O (1246.11 gmol<sup>-1</sup>): C 52.00, H 2.75, N 11.23. Found: C 52.02, H 2.57, N 11.66%. IR ν<sub>max</sub>(neat sample)/cm<sup>-1</sup> 3076, 2951, 1710, 1667, 1625, 1588, 1523, 1479, 1427, 1407, 1372, 1347, 1237, 1196, 1188, 1028, 908, 872, 853, 833, 802, 784, 758, 721, 704, 676.

**[Cu(L<sub>1</sub>)<sub>2</sub>(MeOH)<sub>2</sub>(MeCN)<sub>2</sub>](ClO<sub>4</sub>)<sub>2</sub> (5)**

Ligand L<sub>1</sub> (32 g, 0.1 mmol) was dissolved in 20 mL CH<sub>3</sub>CN/MeOH (1:1). Solid copper(II) perchlorate (18 mg, 0.05 mmol) was added to the pale orange ligand solution resulting in an orange/green solution that was stirred at reflux for 1 hour, before being subjected to vapour diffusion of diethyl ether. Pale green crystals were isolated after careful separation from a pale brown solid (25 mg, 48 %). Anal. Calcd. For [Cu(C<sub>17</sub>H<sub>9</sub>N<sub>3</sub>O<sub>4</sub>)<sub>2</sub>(CH<sub>3</sub>CN)<sub>2</sub>(CH<sub>3</sub>OH)<sub>2</sub>](ClO<sub>4</sub>)<sub>2</sub> (1045.05 gmol<sup>-1</sup>): C 45.88, H 3.08, N 10.70. Found: C 45.65, H 2.63, N 10.22%. IR ν<sub>max</sub>(neat sample)/cm<sup>-1</sup> 3447, 3078, 1718, 1671, 1615, 1583, 1524, 1412, 1373, 1349, 1237, 1197, 1100 (br), 1052, 917, 861, 824, 782, 756, 730, 712, 677.

**Acknowledgements**

We would like to thank, TCD, UCD, IRCSET (JAK Postdoctoral Fellowship) and SFI PI 2010 grant (TG) for financial support to this project.

**Notes and references**

- <sup>a</sup> School of Chemistry, Trinity Biomedical Sciences Institute, Trinity College Dublin, Dublin 2, Ireland. gunnlaut@tcd.ie
- <sup>b</sup> Chemistry, University of Southampton, Southampton, SO17 1BJ, UK. j.a.kitchen@soton.ac.uk
- <sup>c</sup> School of Chemistry and Chemical Biology, University College Dublin, Belfield, Dublin 4, Ireland.
- <sup>d</sup> Departamento de Química e Bioquímica, CQB, Faculdade de Ciências, Universidade de Lisboa, Campo Grande, 1749-016 Lisboa, Portugal
- <sup>†</sup> Electronic Supplementary Information (ESI) available: [Additional views of packing interactions]. CCDC 958088-958093. See DOI: 10.1039/b000000x/
- <sup>‡</sup> It is known that in the presence of water or in MeOH solutions Cu(II) can be reduced to Cu(I), with the formation of aldehyde. Herein, such reduction was indeed observed, but only for L<sub>2</sub> upon using Cu(CF<sub>3</sub>SO<sub>3</sub>)<sub>2</sub>, giving compound 4, where Bond Valence Sum calculation gave ~1.2. While we do not at present have direct evidence for the nature of this reduction, one could postulate that this is due to the combination of ligand design, and the use of relatively weakly coordinating co-ligands, as in the case of 4, one coordination site is occupied by an CH<sub>3</sub>CN molecule and not by the CF<sub>3</sub>SO<sub>3</sub><sup>-</sup> counter ion as observed in the formation of 3, where the Cu centre is indeed Cu(II).
1. S. Banerjee, E. B. Veale, C. M. Phelan, S. A. Murphy, G. M. Tocci, L. J. Gillespie, D. O. Frimannsson, J. M. Kelly and T. Gunnlaugsson, *Chem. Soc. Rev.*, 2013, **42**, 1601-1618.
2. C. J. McAdam, B. H. Robinson and J. Simpson, *Organometallics*, 2000, **19**, 3644-3653.
3. R. M. Duke, E. B. Veale, F. M. Pfeffer, P. E. Kruger and T. Gunnlaugsson, *Chem. Soc. Rev.*, 2010, **39**, 3936-3953.
4. D. M. L. Goodgame, C. J. Page and I. J. Stratford, *Transition Met. Chem.*, 1991, **16**, 223-229.
5. D. L. Reger, A. Debreczeni and M. D. Smith, *Inorg. Chim. Acta*, 2010, **364**, 10-15.

6. D. L. Reger, J. J. Horger and M. D. Smith, *Chem. Commun.*, 2011, **47**, 2805-2807.
7. D. L. Reger, J. Horger, M. D. Smith and G. J. Long, *Chem. Commun.*, 2009, **41**, 6219-6221.
8. D. L. Reger, J. J. Horger, M. D. Smith, G. J. Long and F. Grandjean, *Inorg. Chem.*, 2011, **50**, 686-704.
9. D. L. Reger, A. Debreczeni, J. J. Horger and M. D. Smith, *Cryst. Growth & Des.*, 2011, **11**, 4068-4079.
10. D. L. Reger, A. Debreczeni and M. D. Smith, *Eur. J. Inorg. Chem.*, 2012, **2012**, 712-719.
11. D. L. Reger, A. Debreczeni and M. D. Smith, *Inorg. Chim. Acta*, 2011, **378**, 42-48.
12. D. L. Reger, J. J. Horger, A. Debreczeni and M. D. Smith, *Inorg. Chem.*, 2011, **50**, 10225-10240.
13. D. L. Reger, A. Debreczeni and M. D. Smith, *Inorg. Chem.*, 2011, **50**, 11754-11764.
14. D. L. Reger, A. Debreczeni, M. D. Smith, J. Jezierska and A. Ozarowski, *Inorg. Chem.*, 2012, **51**, 1068-1083.
15. D. L. Reger, R. F. Semeniuc, J. D. Elgin, V. Rassolov and M. D. Smith, *Cryst. Growth & Des.*, 2006, **6**, 2758-2768.
16. D. L. Reger, J. D. Elgin, R. F. Semeniuc, P. J. Pellechia and M. D. Smith, *Chem. Commun.*, 2005, **32**, 4068-4070.
17. D. L. Reger, E. Sirianni, J. J. Horger, M. D. Smith and R. F. Semeniuc, *Cryst. Growth Des.*, 2010, **10**, 386-393.
18. D. L. Reger, A. Debreczeni, B. Reinecke, V. Rassolov and M. D. Smith, *Inorg. Chem.*, 2009, **48**, 8911-8924.
19. D. L. Reger, B. Reinecke, M. D. Smith and R. F. Semeniuc, *Inorg. Chim. Acta*, 2009, **362**, 4377-4388.
20. D. L. Reger, J. D. Elgin, P. J. Pellechia, M. D. Smith and B. K. Simpson, *Polyhedron*, 2009, **28**, 1469-1474.
21. T. Gunnlaugsson, T. C. Lee and R. Parkesh, *Org. Biomol. Chem.*, 2003, **1**, 3265-3267.
22. T. Gunnlaugsson, H. D. P. Ali, M. Glynn, P. E. Kruger, G. M. Hussey, F. M. Pfeffer, C. M. G. dos Santos and J. Tierney, *J. Fluoresc.*, 2005, **15**, 287-299.
23. T. Gunnlaugsson, M. Glynn, G. M. Tocci, P. E. Kruger and F. M. Pfeffer, *Coord. Chem. Rev.*, 2006, **250**, 3094-3117.
24. S. Banerjee, E. B. Veale, C. M. Phelan, S. A. Murphy, G. M. Tocci, L. J. Gillespie, D. O. Frimannsson, J. M. Kelly and T. Gunnlaugsson, *Chem. Soc. Rev.* 2013, **42**, 1601 (and references therein).
25. R. M. Duke and T. Gunnlaugsson, *Tetrahedron Lett.*, 2007, **48**, 8043-8047.
26. R. Parkesh, T. C. Lee and T. Gunnlaugsson, *Org. Biomol. Chem.*, 2007, **5**, 310-317.
27. E. B. Veale and T. Gunnlaugsson, *J. Org. Chem.*, 2008, **73**, 8073-8076.
28. G. J. Ryan, S. Quinn and T. Gunnlaugsson, *Inorg. Chem.*, 2008, **47**, 401-403.
29. H. D. P. Ali, P. E. Kruger and T. Gunnlaugsson, *New J. Chem.*, 2008, **32**, 1153-1161.
30. R. B. P. Elmes and T. Gunnlaugsson, *Tetrahedron Lett.*, 2010, **51**, 4082-4087.
31. (a) S. Banerjee, J. A. Kitchen, S. A. Bright, J. E. O'Brien, D. Clive Williams, J. M. Kelly and T. Gunnlaugsson, *Chem. Commun.*, 2013, **49**, 8522. (b) S. Banerjee, J. A. Kitchen, T. Gunnlaugsson and J. M. Kelly, *Org. Biomol. Chem.*, 2013, **11**, 5642. (c) S. Banerjee, J. A. Kitchen, T. Gunnlaugsson and J. M. Kelly, *Org. Biomol. Chem.*, 2012, **10**, 3033-3043.
32. R. B. P. Elmes, M. Erby, S. A. Bright, D. C. Williams and T. Gunnlaugsson, *Chem. Commun.*, 2012, **48**, 2588-2590.
33. E. B. Veale, J. A. Kitchen and T. Gunnlaugsson, *Supramol. Chem.*, 2013, **25**, 101-108.
34. E. B. Veale, D. O. Frimannsson, M. Lawler and T. Gunnlaugsson, *Org. Lett.*, 2009, **11**, 4040-4043.
35. E. B. Veale and T. Gunnlaugsson, *J. Org. Chem.*, 2010, **75**, 5513-5525.
36. M. Daszkiewicz, *CrystEngComm.*, 2013, **15**, 10427-10430.
37. A. W. Addison, T. N. Rao, J. Reedijk, J. van Rijn and G. C. Verschoor, *J. Chem. Soc., Dalton Trans*, 1984, **7**, 1349-1356.
38. E. I. Solomon and A. B. P. Lever, *Inorganic Electronic Structure and Spectroscopy*, John Wiley & Sons, New York, 2006, vol. 2.
39. J. E. Weder, T. W. Hambley, B. J. Kennedy, P. A. Lay, D. MacLachlan, R. Bramley, C. D. Delfs, K. S. Murray, B. Moubaraki, B. Warwick, J. R. Biffin and H. L. Regtop, *Inorg. Chem.*, 1999, **38**, 1736-1744.
40. D. Kovala-Demertzi, D. Skrzypek, B. Szymańska, A. Galani and M. A. Demertzis, *Inorg. Chim. Acta*, 2005, **358**, 186-190.
41. G. M. Sheldrick, *Acta Crystallogr., Sect. A: Found. Crystallogr.*, 2008, **A64**, 112-122.

Table 1. Crystallographic data and parameters.

	[L <sub>1</sub> -Br]	[L <sub>2</sub> -Br]-MeCN	[Cu <sub>2</sub> (L <sub>1</sub> )(OAc) <sub>2</sub> ](1)	[Cu <sub>2</sub> (L <sub>2</sub> )(OAc) <sub>2</sub> ]-2MeCN (2)	[Cu(L <sub>3</sub> ) <sub>2</sub> MeCN](CF <sub>3</sub> SO <sub>3</sub> ) (4)	[Cu(L <sub>2</sub> )(MeOH) <sub>2</sub> (MeCN) <sub>2</sub> ](ClO <sub>4</sub> ) <sub>2</sub> (5)	
Empirical formula	C <sub>29</sub> H <sub>16</sub> N <sub>4</sub> O <sub>4</sub> Br	C <sub>29</sub> H <sub>16</sub> N <sub>4</sub> O <sub>4</sub> Br	C <sub>29</sub> H <sub>16</sub> N <sub>4</sub> O <sub>4</sub> Br	C <sub>29</sub> H <sub>16</sub> N <sub>4</sub> O <sub>4</sub> Br	C <sub>29</sub> H <sub>16</sub> N <sub>4</sub> O <sub>4</sub> Br	C <sub>29</sub> H <sub>16</sub> N <sub>4</sub> O <sub>4</sub> Br	
Formula weight	490.31	531.36	1640.34	1083.91	1211.48	1047.18	
Temperature	108(2) K	123(2) K	108(2) K	108(2) K	121(2) K	108(2) K	
Wavelength	0.71073 Å	0.71073 Å	0.71073 Å	0.71073 Å	0.71073 Å	0.71073 Å	
Crystal system	Monoclinic	Monoclinic	Triclinic	Triclinic	Triclinic	Monoclinic	
Space group	C2/c	P2 <sub>1</sub> /n	P-1	P-1	P-1	P2 <sub>1</sub> /c	
Unit cell dimensions	a = 29.27(6) Å, α = 90° b = 9.062(2) Å, β = 103.34(3)° c = 15.263(3) Å, γ = 90°	a = 7.252(2) Å, α = 90° b = 25.162(5) Å, β = 102.23(3)° c = 12.801(3) Å, γ = 90°	a = 8.791(2) Å, α = 101.78(3)° b = 9.799(2) Å, β = 95.46(3)° c = 20.206(4) Å, γ = 99.72(3)°	a = 8.739(2) Å, α = 99.75(3)° b = 9.088(2) Å, β = 94.30(3)° c = 17.536(4) Å, γ = 118.30(3)°	a = 11.966(2) Å, α = 109.59(3)° b = 14.668(3) Å, β = 103.35(3)° c = 15.581(3) Å, γ = 93.41(3)°	a = 15.707(3) Å, α = 90° b = 8.125(2) Å, β = 99.55(3)° c = 16.943(3) Å, γ = 90°	a = 15.707(3) Å, α = 90° b = 8.125(2) Å, β = 99.55(3)° c = 16.943(3) Å, γ = 90°
Volume	4174.8(15) Å <sup>3</sup>	2282.6(8) Å <sup>3</sup>	1664.1(6) Å <sup>3</sup>	1189.0(4) Å <sup>3</sup>	2478.8(9) Å <sup>3</sup>	2132.2(7) Å <sup>3</sup>	
Z	8	4	1	1	2	2	
Density (calculated)	1.560 Mg/m <sup>3</sup>	1.546 Mg/m <sup>3</sup>	1.637 Mg/m <sup>3</sup>	1.514 Mg/m <sup>3</sup>	1.623 Mg/m <sup>3</sup>	1.631 Mg/m <sup>3</sup>	
Absorption coefficient	2.007 mm <sup>-1</sup>	1.843 mm <sup>-1</sup>	0.738 mm <sup>-1</sup>	0.975 mm <sup>-1</sup>	0.580 mm <sup>-1</sup>	0.728 mm <sup>-1</sup>	
F(000)	1984	1080	838	554	1232	1070	
Crystal size	0.30 x 0.26 x 0.24 mm <sup>3</sup>	0.32 x 0.25 x 0.17 mm <sup>3</sup>	0.34 x 0.18 x 0.14 mm <sup>3</sup>	0.35 x 0.26 x 0.24 mm <sup>3</sup>	0.43 x 0.22 x 0.06 mm <sup>3</sup>	0.40 x 0.40 x 0.20 mm <sup>3</sup>	
Theta range for data collection	2.54 to 25.00° -31° ≤ h ≤ 34, -11° ≤ k ≤ 9, -18° ≤ l ≤ 18	1.62 to 25.00° -8° ≤ h ≤ 8, -13° ≤ k ≤ 29, -9° ≤ l ≤ 15	3.01 to 25.00° -10° ≤ h ≤ 10, -11° ≤ k ≤ 11, -24° ≤ l ≤ 24	2.61 to 24.49° -7° ≤ h ≤ 10, -10° ≤ k ≤ 9, -20° ≤ l ≤ 20	1.44 to 25.00° -14° ≤ h ≤ 14, -17° ≤ k ≤ 17, -18° ≤ l ≤ 18	2.57 to 25.50° -19° ≤ h ≤ 19, -9° ≤ k ≤ 9, -20° ≤ l ≤ 20	
Reflections collected	16553	8104	26049	7727	28442	17603	
Independent reflections	3649 [R(int) = 0.0934]	3866 [R(int) = 0.0497]	5862 [R(int) = 0.0381]	3766 [R(int) = 0.0994]	8359 [R(int) = 0.0380]	3940 [R(int) = 0.0249]	
Completeness to theta = 25.00°	99.0 %	96.0 %	99.8 %	95.1 %	95.7 %	99.1 %	
Absorption correction	Semi-empirical from equivalents	Semi-empirical from equivalents	Semi-empirical from equivalents	Semi-empirical from equivalents	Semi-empirical from equivalents	Semi-empirical from equivalents	
Max. and min. transmission	0.6444 and 0.5842	1.0000 and 0.4225	0.9037 and 0.7875	0.8004 and 0.7275	1.0000 and 0.5890	1.0000 and 0.7948	
Refinement method	Full-matrix least-squares on F <sup>2</sup>	Full-matrix least-squares on F <sup>2</sup>	Full-matrix least-squares on F <sup>2</sup>	Full-matrix least-squares on F <sup>2</sup>	Full-matrix least-squares on F <sup>2</sup>	Full-matrix least-squares on F <sup>2</sup>	
Data / restraints / parameters	3649 / 0 / 309	3866 / 0 / 319	5862 / 2 / 568	3766 / 1 / 356	8359 / 9 / 778	3940 / 0 / 315	
Goodness-of-fit on F <sup>2</sup>	1.131	1.130	1.097	1.209	1.181	1.183	
Final R indices [I ≥ 2σ(I)]	R <sub>1</sub> = 0.0764, wR <sub>2</sub> = 0.1729	R <sub>1</sub> = 0.0885, wR <sub>2</sub> = 0.2217	R <sub>1</sub> = 0.0433, wR <sub>2</sub> = 0.0988	R <sub>1</sub> = 0.1200, wR <sub>2</sub> = 0.3304	R <sub>1</sub> = 0.0774, wR <sub>2</sub> = 0.1845	R <sub>1</sub> = 0.0322, wR <sub>2</sub> = 0.1054	
R indices (all data)	R <sub>1</sub> = 0.1115, wR <sub>2</sub> = 0.1943	R <sub>1</sub> = 0.1003, wR <sub>2</sub> = 0.2315	R <sub>1</sub> = 0.0483, wR <sub>2</sub> = 0.1019	R <sub>1</sub> = 0.1355, wR <sub>2</sub> = 0.3505	R <sub>1</sub> = 0.0837, wR <sub>2</sub> = 0.1888	R <sub>1</sub> = 0.0396, wR <sub>2</sub> = 0.1296	
Largest diff. peak and hole	0.730 and -0.469 e.Å <sup>-3</sup>	1.482 and -0.648 e.Å <sup>-3</sup>	0.537 and -0.381 e.Å <sup>-3</sup>	0.998 and -1.211 e.Å <sup>-3</sup>	0.638 and -0.585 e.Å <sup>-3</sup>	0.449 and -0.439 e.Å <sup>-3</sup>	

## ARTICLE

**Synthesis, crystal structure and EPR spectroscopic analysis of novel copper complexes formed from N-pyridyl-4-nitro-1,8-naphthalimide ligands**

Jonathan A. Kitchen, Paulo N. Martinho, Grace G. Morgan, and Thorfinnur Gunnlaugsson

The synthesis of two new monodentate pyridyl based 4-nitro-1,8-naphthalimide ligands and their corresponding Cu-complexes (using various salts) is described. Of these, complexes **1-3** and **5**, all gave rise to structures that were characterised by X-ray crystallography and EPR.

